

Exact rate calculations by trajectory parallelization and twisting

Eric Vanden-Eijnden^{1,*} and Maddalena Venturoli^{1,†}

¹*Courant Institute of Mathematical Sciences, New York University, New York, NY 10012, USA*

(Dated: June 13, 2022)

A sampling procedure to compute exactly the rate of activated processes arising in systems at equilibrium or nonequilibrium steady state is presented. The procedure is a generalization of the method in [A. Warmflash, P. Bhimalapuram, and A. R. Dinner, J. Chem. Phys. **127**, 154112 (2007); A. Dickson, A. Warmflash, and A. R. Dinner, J. Chem. Phys. **130**, 074104 (2009)] in which one performs simulations restricted into cells by using a reinjection rule at the boundaries of the cells which is consistent with the exact probability fluxes through these boundaries. Our generalization uses results from transition path theory which indicate how to twist the dynamics to calculate reaction rates.

PACS numbers: 02.50.-r, 02.60.-x, 31.15.xv, 82.20.Pm

Keywords: statistical steady state; Voronoi tessellation; reactive trajectories; Markovian dynamics; milestone-ing

Introduction. The main objective of this work is to revisit and extend in scope the nonequilibrium sampling procedure to compute steady state probability distributions proposed in Refs. 1,2. Specifically, we show how this procedure can be modified to calculate exactly certain dynamical quantities such as the rate of reactions occurring in arbitrary equilibrium or nonequilibrium systems at statistical steady state. This is done by exploiting results of transition path theory (TPT)^{3,4,5} which indicate how to twist the dynamics of a given system to calculate the reaction rate between a given reactant and product state. The method proposed in this note can be seen as a generalization to arbitrary nonequilibrium processes at statistical steady state of the milestoneing procedure with Voronoi tessellation proposed in Ref. 6 by building upon the original works in Refs. 7,8,9. This generalization makes the procedure more expensive computationally, but it permits to relax completely the assumptions made in milestoneing – these assumptions were discussed in detail in Ref. 10. Our method can also be viewed as a generalization of the transition interface sampling (TIS)^{11,12,13} and forward flux sampling (FFS)^{14,15} methods in which arbitrary sets of interfaces can be used that do not have to be placed in monotone succession.

The remainder of this note is organized as follows. First we revisit from an original perspective the nonequilibrium sampling procedure of Refs. 1,2. Next, we show how this procedure can be modified to calculate reaction rates exactly using TPT. We then compare our procedure with the Markovian milestoneing method proposed in Ref. 6 and with TIS^{11,12,13} and FFS^{14,15}. Finally we illustrate our procedure on a simple example. In terms of notations and assumptions, we will denote by \mathbf{z} the location of the system in its state-space $\Omega \subset \mathbb{R}^d$ (e.g. it could be the positions and velocities of all the atoms in a molecular system, in which case $\mathbf{z} = (\mathbf{x}, \mathbf{v})$ and $d = 6n$ if n is the number of atoms). The specifics of the dynamics of the system are not important except that we assume that (i) its evolution is Markovian and (ii) it is ergodic with respect to a probability density function which we

denote by $\varrho(\mathbf{z})$. Notice that we do not require detailed balance, i.e. $\varrho(\mathbf{z})$ is associated with a nonequilibrium statistical steady state in general.

Restricted sampling with flux matching. The methods in Refs. 1,2,6 are based on a factorization of the dynamics in which one artificially constrains the system to evolve in a set of cells partitioning state-space in a way that (i) does not bias the dynamics inside the cells and (ii) is consistent with the exact probability fluxes in and out of these cells. In other words, the procedure guarantees that a true unconstrained trajectory of the system can be reconstructed exactly by patching together in some appropriate way the pieces computed in the cells. These pieces can be calculated in parallel in each cell, hence the name trajectory parallelization. The method in Ref. 6 is restricted to equilibrium systems and exploits the time-reversibility of the dynamics. The method in Refs. 1,2 is more costly but it works also for nonequilibrium systems. To explain how the latter method works, we first recall how to construct the cells using the Voronoi tessellation associated with a given set of generating points or centers^{6,16}. Denoting these centers by $\mathbf{z}_\alpha \in \Omega \subset \mathbb{R}^d$, with $\alpha = 1, \dots, \Lambda$, the Voronoi cell B_α associated to \mathbf{z}_α contains all the points that are closer to \mathbf{z}_α than to any other center, i.e. (see Fig. 1 for an illustration)

$$B_\alpha = \{\mathbf{z} \in \Omega : \|\mathbf{z} - \mathbf{z}_\alpha\| < \|\mathbf{z} - \mathbf{z}_\beta\| \text{ for all } \beta \neq \alpha\}, \quad (1)$$

where $\|\cdot\|$ is some appropriate norm (e.g. the Euclidean norm in which case $\|\mathbf{z}\|^2 = \sum_{i=1}^d z_i^2$).

If we were to generate an infinitely long trajectory of the system, $\mathbf{z}(t)$ with $t > 0$, this trajectory would keep going in and out of the cells B_α by crossing the edges between these cells. Out of this trajectory we could therefore generate an ensemble of exit-entry points, i.e. those points on the edges of the cells at which the trajectory goes from a cell B_α into a neighboring cell B_β . By the Markovian assumption, these points are all we need to generate an exact sample of trajectories inside each of the cells B_α simply by starting trajectories at the points leading into that cell and running these trajectories for-

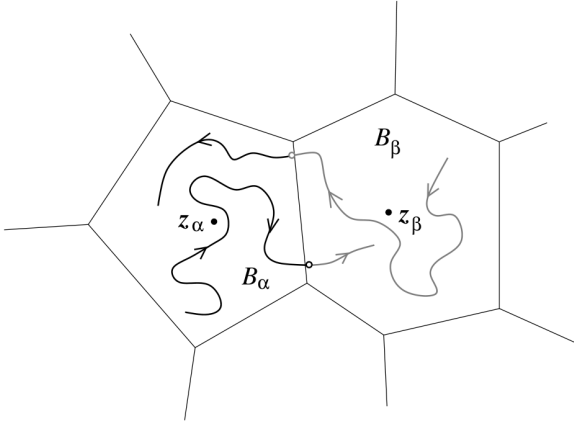


FIG. 1: Representation of a portion of the Voronoi tessellation in two-dimension, where point z_α is the generator of cell B_α and point z_β the generator of cell B_β . Pieces of restricted trajectory inside B_α are shown in black and inside B_β in grey. Each time the trajectory in one cell attempts to exit the cell, the exit point position (depicted as an open circle) is stored, and used to reinitialize the trajectory into the neighboring cell.

ward in time until they exit the cell. The procedure in Refs. 1,2 is a way to generate these pieces of trajectories inside the cells without having to compute the entry points beforehand from a long unbiased trajectory but rather by generating them on-the-fly. To understand how this is done, imagine that we associate an independent copy, or replica, of the system to each cell B_α . Let us denote the instantaneous position of these replicas by $z_\alpha(t) \in B_\alpha$, $\alpha = 1, \dots, \Lambda$. Even if we start $z_\alpha(t)$ inside B_α , sooner or later this trajectory will try to exit B_α and go to another cell. When this happens, we store the exit point on the boundary, put the trajectory on hold and wait until a trajectory in one of the neighboring cells makes an attempt to exit this cell by crossing the boundary with B_α . We then take this crossing point and use it to reinitialize the trajectory in B_α . This is illustrated in Fig. 1. At the beginning of the simulation we do not have enough re-entry points, so many of the replicas may be on hold. But as the simulation goes on, we can build databanks of re-entry points from any B_β into any B_α (assuming that these two cells have a common boundary – otherwise the databank is trivially empty), which contain the last X points by which the trajectory tried to escape from cell B_β and enter cell B_α . This way, each time a trajectory tries to exit a cell B_α , we can immediately pick a re-entry point into that cell from the appropriate databank and continue the trajectory from that point without having to put it on hold.

The only remaining issue we need to take care of in order to make complete the procedure outlined above is how to pick the re-entry point into B_α among the databanks on the various edges leading into B_α . By construction, the re-entry points in the databanks on each edge are unbiased samples of re-entry points conditional

on the trajectory entering by that edge. But there are several edges by which the trajectory can enter a given cell, and to introduce no bias we need to pick the edges with the proper probability of re-entrance by that edge. To see how this can be done, imagine that, as we run the simulation in each cell B_α , we compute an estimate of the effective rate of exit out that cell and into B_β via

$$\nu_{\alpha,\beta} = \frac{N_{\alpha,\beta}}{T_\alpha} \quad (2)$$

where $N_{\alpha,\beta}$ is the total number of times the trajectory hit the boundary between B_α and B_β (which is also the number of times the trajectory in cell B_α had to be re-injected into that cell from a re-entry point) and T_α is the total simulation time in cell B_α (i.e. the total time the trajectory in cell B_α was running). If we then denote by π_α the probability to find the unbiased trajectory inside cell B_α at statistical steady state, i.e.

$$\pi_\alpha = \int_{B_\alpha} \varrho(z) dz, \quad (3)$$

we see that π_α and $\nu_{\alpha,\beta}$ are related as

$$\sum_{\substack{\beta=1 \\ \beta \neq \alpha}}^{\Lambda} \pi_\beta \nu_{\beta,\alpha} = \sum_{\substack{\beta=1 \\ \beta \neq \alpha}}^{\Lambda} \pi_\alpha \nu_{\alpha,\beta}, \quad \sum_{\alpha=1}^{\Lambda} \pi_\alpha = 1. \quad (4)$$

The first equation in (4) simply expresses that, at statistical steady state, the total probability flux into B_α (which is the term at the left hand-side of the first equation in (4)) must be equal to the total flux out of B_α (which is the term at the right hand-side of the first equation in (4)). The second equation in (4) is simply a normalization condition for the probability which follows from $\sum_\alpha \pi_\alpha = \sum_\alpha \int_{B_\alpha} \varrho(z) dz = \int_\Omega \varrho(z) dz = 1$. We stress that (4) does not require detailed balance (i.e. $\pi_\beta \nu_{\beta,\alpha} \neq \pi_\alpha \nu_{\alpha,\beta}$, possibly) and so it holds even for nonequilibrium processes provided only that they are at statistical steady state. Having calculated $\nu_{\alpha,\beta}$ from (2) and π_α from (4), we then have an estimate for the probability flux from B_β into B_α : $\pi_\beta \nu_{\beta,\alpha}$. Consistently, the probability that the trajectory enters cell B_α by coming from B_β is simply:

$$\mathbb{P}_{\partial B_\beta \cap \partial B_\alpha} = \frac{\pi_\beta \nu_{\beta,\alpha}}{\sum_{\beta' \neq \alpha} \pi_{\beta'} \nu_{\beta',\alpha}}, \quad (\beta \neq \alpha), \quad (5)$$

if B_α and B_β have a common edge and $\mathbb{P}_{\partial B_\beta \cap \partial B_\alpha} = 0$ otherwise. This expression gives us the desired probability to pick the edge $\partial B_\beta \cap \partial B_\alpha$ for re-entry into B_α .

Summarizing, the algorithm to perform simulations restricted inside the cells for systems at nonequilibrium steady state is as follows:

- (1) Denoting by $z_\alpha(t) \in B_\alpha$ the current state of the replica in cell B_α , let z_α^* be the state of the system produced from $z_\alpha(t)$ after one timestep Δt by

a standard (i.e. unrestricted) integrator for the system (e.g. velocity-Verlet if the system is a molecular dynamics (MD) system). If $\mathbf{z}_\alpha^* \in B_\alpha$, set

$$\mathbf{z}_\alpha(t + \Delta t) = \mathbf{z}_\alpha^*. \quad (6)$$

Otherwise, if $\mathbf{z}_\alpha^* \in B_\beta$ with $\beta \neq \alpha$:

- (i) Store the point \mathbf{z}_α^* in a databank of entry points from B_α into B_β . In other words, assuming that the databank contains already m points $\mathbf{z}_{\alpha,\beta}^k$ with $k = 1, 2, \dots, m$, set $\mathbf{z}_{\alpha,\beta}^{m+1} = \mathbf{z}_\alpha^*$.
- (ii) Update $\nu_{\alpha,\beta}$ via (2), π_α via (4) and $\mathbb{P}_{\partial B_\beta \cap \partial B_\alpha}$ via (5).
- (iii) Select an edge $\partial B_{\beta'} \cap \partial B_\alpha$ of B_α with probability proportional to $\mathbb{P}_{\partial B_{\beta'} \cap \partial B_\alpha}$.
- (iv) Pick a point $\mathbf{z}_{\beta',\alpha}^k$ with uniform probability from the databank of re-entry points on edge $\partial B_{\beta'} \cap \partial B_\alpha$, and set

$$\mathbf{z}_\alpha(t + \Delta t) = \mathbf{z}_{\beta',\alpha}^k \quad (7)$$

- (2) Go to step (1) and iterate to collect statistics.

In essence, the algorithm above is the same as the one proposed in Ref. 1,2, though the two differ in the details. For instance, we use a single set of cells instead of two (in Refs. 1,2 two staggered sets were used to ensure stability, but we observed no such stability problems with the procedure above). Besides a set of trajectories, one of the output of the procedure is to give the probability π_α to find the system in cell B_α at statistical steady state (see (3)). Indeed the computation of π_α was the main objective in Refs. 1,2. Below we will show how to extract more from the procedure, in particular reaction rate information, by appropriate modifications. Before getting there, however, let us make a few remarks about the algorithm above. In step (iv) we have assumed that the list of entry points from $B_{\beta'}$ into B_α is not empty and, as already mentioned above, this may not be true at the beginning of the simulation (there might have been no collision with that edge up to that time). In that case we have to put the simulations in some of cells on hold at the beginning until we get proper re-entry points and start building databanks on the edges. Note that, at any given time, these databanks could each contain the last re-entry point only, though in that case we may run out of points again and have to put replicas on hold. Thus it is safer to always keep as many points in the databanks as memory allows. However, the databanks do not have to be enlarged indefinitely – at worst we trade memory for CPUs since, the smaller the databanks, the higher the probability that one replica will have to be put on hold for some time. Also note that the quantities used to evaluate the probability in Eq. (5) have to be computed on-the-fly, and need information from all the cells. This, again, may lead to problems at the beginning of the simulations, when the statistics for $N_{\alpha,\beta}$ is

not accurate enough. To overcome this problem we set $\pi_\alpha = cst \ \forall \alpha = 1, \dots, N$ at the beginning when statistics is insufficient to solve Eq. (4). Using more educated guesses is possible too. Also, it is worth noting that $\nu_{\alpha,\beta}$ and π_α can be monitored on-the-fly to assess their convergence as a function of the length of the simulation, and the actual simulations of the replicas in each cell can be performed in parallel; only the re-entry events require communication. Finally, we should stress that the procedure above relies on the ability to count the successive points at which a trajectory crosses the edges of the cells. This may lead to difficulties if the dynamics is governed by a stochastic differential equation, in which case these crossing points may form a fractal set. It leads to no difficulty, however, if some components of the trajectory are smooth and the cells are defined accordingly. We will come back to this issue later in the illustrative example section.

Rate calculation. Let us now come to the question of how to compute the reaction rate between a reactant and product state, which we identify as two disjoint sets in the system's state-space denoted as $A \subset \Omega$ and $B \subset \Omega$ respectively. As mentioned earlier, this calculation will be done by twisting the dynamics in some appropriate way that is dictated by the results of TPT. We begin by introducing the relevant objects that we will consider. If we assume again that we have at our disposal an infinitely long trajectory, $\mathbf{z}(t)$ with $t > 0$, this trajectory will go back and forth between A and B as time goes on, and we can split this trajectory into two pieces, depending on whether it visited last A or B . This construction is illustrated in Fig. 2, where the trajectory is shown in red if it visited A last and in black if it visited B last: if the trajectory visited A last at time t , we will say that it is assigned to A at time t , if it visited B last at time t , we will say that it is assigned to B at time t .

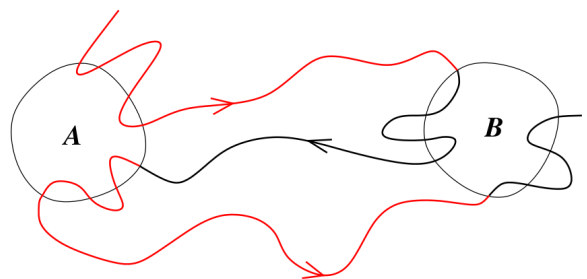


FIG. 2: Schematic representation of a piece of ergodic trajectory visiting the two sets A and B . The pieces of this trajectory for which the last visited set was A are depicted in red, and those for which the last visited set was B are depicted in black.

Based on this assignment, we can introduce the following quantities. If $N_{A,B}^T$ denotes the total number of times the trajectory went from being assigned to A to being assigned to B during the time interval $[0, T]$ (i.e. the number of times it switched from red to black in Fig. 2),

we set

$$\nu_R = \lim_{T \rightarrow \infty} \frac{N_{A,B}^T}{T}. \quad (8)$$

This quantity gives the average frequency at which the trajectory goes from A to B which, because the system is at steady state, is also the same as the average frequency at which the trajectory goes from B to A since $N_{A,B}^T = N_{B,A}^T$ asymptotically. The rate in (8) is referred to as the rate of the reactive trajectories in TPT, hence the subscript R . The rate of reactive trajectories ν_R should not be confused with the two reaction rates from A to B and B to A defined respectively as

$$k_{A,B} = \lim_{T \rightarrow \infty} \frac{N_{A,B}^T}{T_A}, \quad k_{B,A} = \lim_{T \rightarrow \infty} \frac{N_{A,B}^T}{T_B}, \quad (9)$$

where T_A and T_B are, respectively, the total times during which the trajectory was assigned to A or B in the interval $[0, T]$ (i.e. the total times the trajectory is red or black in Fig. 2). If A and B are metastable (i.e. if the trajectory commits to each of these sets and loses memory of its past before going back to the other set), $k_{A,B}$ and $k_{B,A}$ are the rates that enter the phenomenological mass-action law describing how the populations in A and B evolve in time. Notice that ν_R is related to $k_{A,B}$ and $k_{B,A}$ as

$$k_{A,B} = \frac{\nu_R}{\rho_A}, \quad k_{B,A} = \frac{\nu_R}{\rho_B}, \quad (10)$$

where ρ_A is the fraction of time the trajectory is assigned to A and ρ_B the fraction of time it is assigned to B :

$$\rho_A = \lim_{T \rightarrow \infty} \frac{T_A}{T}, \quad \rho_B = \lim_{T \rightarrow \infty} \frac{T_B}{T}. \quad (11)$$

By definition $\rho_A \leq 1$, $\rho_B \leq 1$ and $\rho_A + \rho_B = 1$. The quantities ν_R , $k_{A,B}$, $k_{B,A}$, ρ_A and ρ_B are the ones we will show how to compute exactly. To see how this can be done, it is useful to give first the TPT expressions for these quantities. These expressions involve the backward committor function, $q_-(\mathbf{z})$, which gives the probability that a trajectory observed at point \mathbf{z} is coming from A last rather than from B (i.e. that it is assigned to A rather than B using the jargon introduced above). By definition $q_-(\mathbf{z}) = 1$ if $\mathbf{z} \in A$, $q_-(\mathbf{z}) = 0$ if $\mathbf{z} \in B$, and $0 \leq q_-(\mathbf{z}) \leq 1$ otherwise. The backward committor function is useful because by the Markovian assumption it follows that, at statistical steady state, the probability density to observe a trajectory at point $\mathbf{z} \in \Omega$ at any given time t and that this trajectory is assigned to A at that time is simply $\varrho_A(\mathbf{z}) = \varrho(\mathbf{z}) q_-(\mathbf{z})$. Similarly the probability density to observe a trajectory at point $\mathbf{z} \in \Omega$ at time t and that this trajectory is assigned to B at that time is $\varrho_B(\mathbf{z}) = 1 - \varrho_A(\mathbf{z}) = \varrho(\mathbf{z}) (1 - q_-(\mathbf{z}))$. Since $\rho_A = \int_{\Omega} \varrho_A(\mathbf{z}) d\mathbf{z}$ and $\rho_B = \int_{\Omega} \varrho_B(\mathbf{z}) d\mathbf{z}$ by definition, this implies that

$$\rho_A = \int_{\Omega} \varrho(\mathbf{z}) q_-(\mathbf{z}) d\mathbf{z} \leq 1, \quad \rho_B = 1 - \rho_A. \quad (12)$$

Similarly, it is easy to see that ν_R is the total probability flux associated with $\varrho_A(\mathbf{z}) = \varrho(\mathbf{z}) q_-(\mathbf{z})$ going through any dividing surface between A and B (like e.g. the boundary of B). The explicit form of this flux depends on the specifics of the dynamics and it is given in Ref. 4: let us omit to repeat this formula here since it will not be important in what follows.

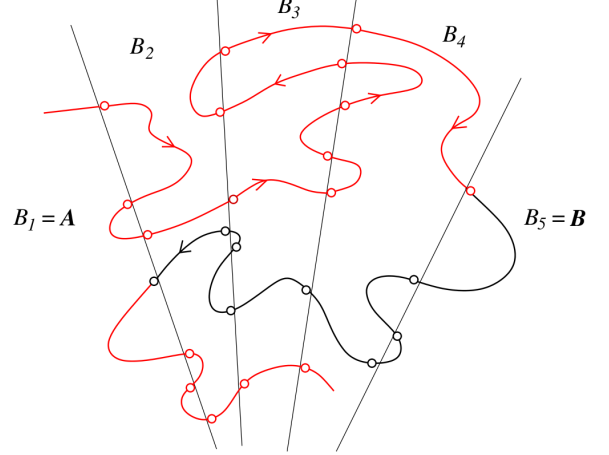


FIG. 3: Schematic illustration of a piece of trajectory crossing the cells B_α with $\alpha = 1, \dots, 5$, where cell B_1 is identified with the reactant state A and cell B_5 with the product state B . The circles represent the entry points which would be used to perform sampling restricted in the cells. If only the red points are used as re-entry points, then the restricted sampling selects the pieces of this trajectory when it is assigned to A (these pieces are depicted in red).

In practice, we do not know explicitly $q_-(\mathbf{z})$ (nor even $\varrho(\mathbf{z})$ in most nonequilibrium systems) but we can still make use of the observations above to modify the sampling procedure explained before. Suppose that we define the reactant state A as being the union of a group of cells B_α and the product state B as the union of another group. Clearly, what we would then like to do is modify the sampling procedure in such a way that only the re-entry points associated with the trajectory when it is assigned to A are put in the databanks (see the illustration in Fig. 3) and keep track of the associated probability fluxes through the boundary of the cells. Indeed, using these re-entry points and these fluxes only, we would then simulate in the cells pieces of trajectories that are statistically indistinguishable from the unbiased trajectory when it is assigned to A . We could then compute the total probability in the cells to get an estimate of ρ_A (and hence $\rho_B = 1 - \rho_A$) as well as the total flux into B to get ν_R . We claim that there is a simple procedure to do these operations in practice. The key observation is that trajectories assigned to A can be propagated like regular trajectories while they are outside of A and B – the only constraint imposed on them is via a boundary condition in their past: they need to have come from A rather than B last. But we know what this boundary condition entails, at least in a statistical sense: indeed

the probability density $\varrho_A(\mathbf{z})$ that a trajectory be at \mathbf{z} and be assigned to A is equal to the statistical steady state probability density $\varrho(\mathbf{z})$ for $\mathbf{z} \in A$ while it is equal to 0 for $\mathbf{z} \in B$. We also know that the probability flux out of A is the statistical steady state one and the probability flux out of B is identically zero.

We can easily impose these boundary conditions in practice by modifying our sampling procedure as follows. Suppose that we have performed a sampling as before and computed the steady state (unbiased) π_α and $\nu_{\alpha,\beta}$. We can then run another independent sampling where we only consider the cells outside of A and B . In these cells, we run trajectories as before (though, as we will see, using re-entry points that are different from the ones calculated before), store their exit points from the cells to build databanks of re-entry points in other cells, and compute

$$\nu_{\alpha,\beta}^A = \frac{N_{\alpha,\beta}^A}{T_\alpha^A} \quad (13)$$

where $N_{\alpha,\beta}^A$ is the total number of times the trajectories hit the boundary between B_α and B_β and T_α^A is the total simulation time in cell B_α . Note that $\nu_{\alpha,\beta}^A$ is only defined by (13) if α is the index of a cell B_α not inside A and B (the index β , on the other hand, runs over all the cells, including those forming A and B). Consistent with the bias we need to impose to focus on trajectories assigned to A , we supplement this by $\nu_{\alpha,\beta}^A = \nu_{\alpha,\beta}$ if α is the index of a cell B_α used to define A (since the effective rate of exit out of A must be the unbiased statistical steady one) and by $\nu_{\alpha,\beta}^A = 0$ if α is the index of a cell B_α used to define B (since the effective rate of exit out of B must be zero). We also set $\pi_\alpha^A = \pi_\alpha$ if α is the index of a cell B_α used to define A , $\pi_\alpha^A = 0$ if α is the index of a cell B_α used to define B , and in all the other cells we compute π_α^A via

$$\sum_{\substack{\beta=1 \\ \beta \neq \alpha}}^{\Lambda} \pi_\beta^A \nu_{\beta,\alpha}^A = \sum_{\substack{\beta=1 \\ \beta \neq \alpha}}^{\Lambda} \pi_\alpha^A \nu_{\alpha,\beta}^A \quad (14)$$

where the index α runs over all the cells outside of A and B and we use as boundary conditions the values for $\nu_{\beta,\alpha}^A$ and π_β^A set before when the index β is that of a cell used to define A or B . Finally, we compute the probability of re-entry on the edges of a cell B_α not inside A and B as

$$\mathbb{P}_{\partial B_\beta \cap \partial B_\alpha}^A = \frac{\pi_\beta^A \nu_{\beta,\alpha}^A}{\sum_{\beta' \neq \alpha} \pi_{\beta'}^A \nu_{\beta',\alpha}^A}, \quad (\beta \neq \alpha). \quad (15)$$

This procedure automatically guarantees that we focus on the trajectories assigned to A and makes all the quantities above – the set of trajectories, the databanks, $\nu_{\alpha,\beta}^A$ and π_α^A – different from their unbiased statistical steady state counterparts. By construction we then have

$\pi_\alpha^A = \int_{B_\alpha} \varrho_A(\mathbf{z}) d\mathbf{z}$ which, from (12), means that

$$\rho_A = \sum_{\alpha=1}^{\Lambda} \pi_\alpha^A \leq 1, \quad \rho_B = 1 - \rho_A. \quad (16)$$

Similarly we can compute ν_R from the total flux into B :

$$\nu_R = \sum_{\substack{\alpha \text{ such that} \\ B_\alpha \text{ not in } B}} \sum_{\substack{\beta \text{ such that} \\ B_\beta \text{ in } B}} \pi_\alpha^A \nu_{\alpha,\beta}^A. \quad (17)$$

Finally, we can get $k_{A,B}$ and $k_{B,A}$ from (10) and be done.

Comparison with TIS, FFS, and Markovian milestone-ing with Voronoi tessellations. Before illustrating our procedure to compute the reaction rate on a simple example, let us point out that it is very similar in spirit to both TIS^{11,12,13} and FFS^{14,15}. Like TIS and FFS, our method is based on selecting only those trajectories which come from the reactant state A . The difference is in the way this selection is achieved. In particular, unlike in TIS and FFS, we do not require that the interfaces be ordered monotonously, i.e. we do not need that a trajectory coming from A crosses all the preceding interfaces before reaching the next one. This offers more flexibility in the way the interfaces can be chosen. Here we did so using the edges of cells in a Voronoi tessellation because it is convenient, but the formalism above is clearly independent of that choice and can be applied to any type of interfaces.

Regarding the relation with the Markovian milestone-ing procedure with Voronoi tessellation⁶, the main advantage of the method proposed in this note to compute the rate is that it is exact and hence avoids completely the assumptions underlying milestone-ing¹⁰. On the other hand, the new procedure is also more costly since it requires not only to build databanks of re-entry points but also to do the sampling twice – once to get the unbiased statistical steady states quantities, and once more to get the reaction rate by twisting the dynamics. For systems at equilibrium, one may therefore prefer to use the Markovian milestone-ing procedure with Voronoi tessellation⁶ which is cheaper. For nonequilibrium systems, this procedure is inapplicable (since it relies on the time-reversibility of the dynamics), but as a compromise, one could use the nonequilibrium sampling strategy for the unbiased system to compute the relevant quantities in Markovian milestone-ing and thereby avoid to make the second twisted sampling to compute the rate. Indeed, the formalism developed in Ref. 6 to approximate the dynamics by a continuous-time Markov chain does not rely on the dynamics being at equilibrium. For completeness let us briefly recall the main objects in Markovian milestone-ing and indicate how to compute them in the present context. If, following Ref. 6, we define the milestones as the common boundaries between any two adjacent Voronoi cells and denote these milestones by S_i with $i = 1, 2, \dots, N$, the key quantity to approximate

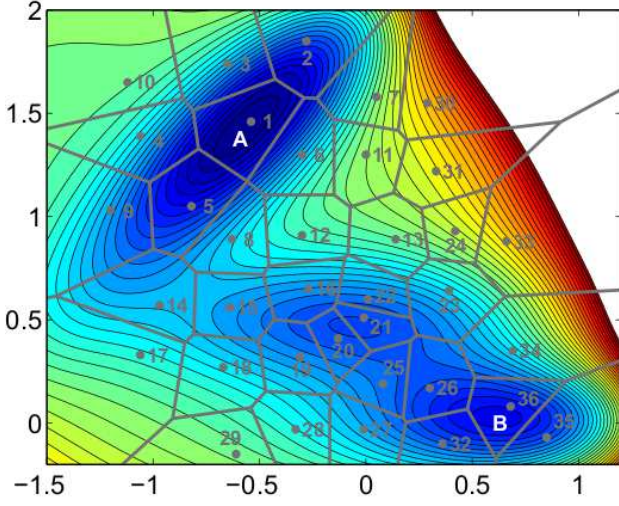


FIG. 4: Contourplot of the Mueller potential with the 36 points (shown as grey dots) generating the Voronoi tessellation shown as grey lines. The reactant A and product B states are identified with cell B_1 and B_{36} , respectively.

the transitions between the milestones by a continuous-time Markov chain is the rate matrix whose off-diagonal elements can be estimated as

$$q_{ij} = \begin{cases} N_{ij}/R_i & \text{if } R_i \neq 0 \\ 0 & \text{if } R_i = 0. \end{cases} \quad (18)$$

where

$$N_{ij} = \sum_{\alpha=1}^{\Lambda} \pi_{\alpha} \frac{N_{ij}^{\alpha}}{T_{\alpha}}, \quad R_i = \sum_{\alpha=1}^{\Lambda} \pi_{\alpha} \frac{R_i^{\alpha}}{T_{\alpha}}. \quad (19)$$

Here T_{α} is the total simulation time in cell B_{α} (as before), whereas N_{ij}^{α} is the total number of times the trajectory went from milestone S_i to milestone S_j and R_i^{α} is the total amount of time the trajectory is assigned to milestone S_i in cell B_{α} , i.e. the total amount of time this trajectory is such that S_i was the edge of cell B_{α} it hit last. We refer the reader to Ref. 6 for more details.

Illustrative example. We end this note by illustrating our sampling procedure on the example of a system evolving by Langevin dynamics on a two-dimensional potential, i.e. $\mathbf{z}(t) = (\mathbf{x}(t), \mathbf{v}(t))$, $\mathbf{x}, \mathbf{v} \in \mathbb{R}^2$ and

$$\begin{cases} \dot{\mathbf{x}}(t) = \mathbf{v}(t), \\ \dot{\mathbf{v}}(t) = -\nabla V(\mathbf{x}(t)) - \gamma \mathbf{v}(t) + \sqrt{2\beta^{-1}\gamma} \boldsymbol{\eta}(t). \end{cases} \quad (20)$$

Here $V(\mathbf{x})$ is the Mueller potential¹⁷ whose contourplot is shown in Fig. 4, $\beta = 1/(k_B T)$ is the inverse temperature and $\boldsymbol{\eta}(t)$ is a Gaussian white-noise with mean zero and covariance $\langle \eta_i(t) \eta_j(t') \rangle = \delta_{ij} \delta(t - t')$. γ is the friction coefficient and, for simplicity, we have set the mass tensor to the identity. Below we took $\gamma = 100$ and $\beta^{-1} = 20$ (which is about 20% the value of the energy barrier between the

minimum at the top left corner of the Mueller potential and the saddle point at $(-0.8, 0.6)$). This example is obviously very simple and serves no other purpose than being a benchmark: the application of our sampling procedure to more interesting examples will be reported elsewhere. To avoid confusions, before presenting our results for (20) let us note that this system is an equilibrium one, with equilibrium density $\varrho(\mathbf{x}, \mathbf{v}) = Z^{-1} \exp(-\beta H(\mathbf{x}, \mathbf{v}))$ where $H(\mathbf{x}, \mathbf{v}) = \frac{1}{2}|\mathbf{v}|^2 + V(\mathbf{x})$ is the Hamiltonian and $Z = \int_{\mathbb{R}^2 \times \mathbb{R}^2} \exp(-\beta H(\mathbf{x}, \mathbf{v})) d\mathbf{x} d\mathbf{v}$ the partition function. We are, however, primarily interested in computing the reaction rates between the reactant state A and the product state B shown in Fig. 4, which we will achieve by twisting the dynamics as explained before to focus on trajectories assigned to A . In so doing, we automatically put the system out of equilibrium since A becomes a source and B a sink (and $\varrho_A(\mathbf{x}, \mathbf{v}) \neq \varrho(\mathbf{x}, \mathbf{v})$). This is why we need the nonequilibrium formalism developed above to compute reaction rates even in the case of an equilibrium system such as (20).

Shown in Fig. 4 are the 36 cells that we used in our calculations. These cells were defined as

$$B_{\alpha} = \{(\mathbf{x}, \mathbf{v}) \in \mathbb{R}^2 \times \mathbb{R}^2 : |\mathbf{x} - \mathbf{x}_{\alpha}| < |\mathbf{x} - \mathbf{x}_{\beta}| \text{ for all } \beta \neq \alpha\}, \quad (21)$$

where $|\cdot|$ denotes the Euclidean norm and \mathbf{x}_{α} with $\alpha = 1, \dots, 36$ are points chosen randomly in the region where the energy is below a certain threshold value. We identified the reactant and product states with two single cells in the neighborhood of the two deep minima in the potential landscape: $A = B_1$ and $B = B_{36}$ (see Fig 4). Note that we intentionally took many cells and disposed them in a way that may not be optimal for the reaction to check that our procedure is robust against such choices. Note also that by defining the cells primarily in position space as we do in (21) we guarantee that we can count successive crossing of their boundaries. This would not be the case if the boundaries of the cells were bent in velocity space, because of the noise term in (20) that acts on the velocities.

Both steps of the sampling procedure (the one to compute the unbiased equilibrium quantities and the other with the twisted dynamics) were performed as described above by running simulations for 10^8 steps in each cell using the second order integrator of Ref. 18 with a timestep $\Delta t = 10^{-4}$. In the first step of the procedure we took π_{α} equal in each cell as initial condition; in the second step, we took $\pi_{\alpha}^A = \pi_{\alpha}$ as initial condition. We compared the results of our procedure with those obtained by generating a long (10^{10} steps) unbiased trajectory by brute force simulation and computing ν_R , $k_{A,B}$ and $k_{B,A}$ from finite T approximations of the limits in (8) and (9).

The main outputs of our procedure are the rate of reactive trajectories ν_R and the reaction rates $k_{A,B}$ and $k_{B,A}$ which are reported in Table I. These are within statistical errors of the corresponding quantities estimated by brute force simulation. Our procedure also produces the equilibrium probabilities π_{α} : as shown in Fig. 5 these

	ν_R	$k_{A,B}$	$k_{B,A}$
Twisted dynamics	$5.9 \cdot 10^{-3}$	$7.4 \cdot 10^{-3}$	$3.1 \cdot 10^{-3}$
Direct simulation	$5.8 \cdot 10^{-3}$	$7.1 \cdot 10^{-3}$	$3.2 \cdot 10^{-3}$

TABLE I: Rate of reactive trajectories and reaction rates between the sets A and B in the Mueller potential (see Fig. 4) obtained by the procedure presented here and by direct calculation using a long unbiased trajectory.

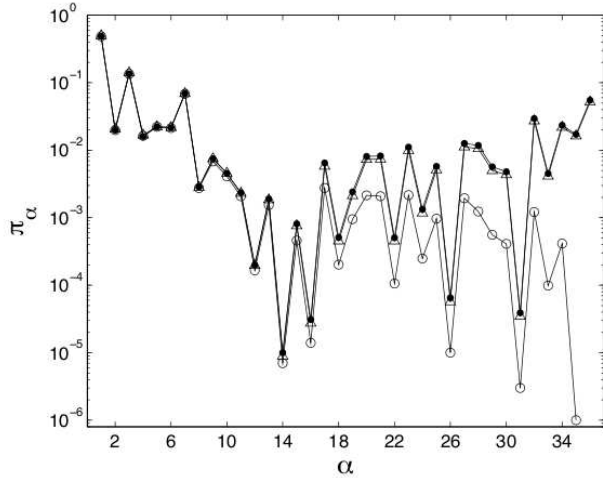


FIG. 5: Probability π_α to be in the cells (semi-log scale) obtained via sampling restricted in the Voronoi cells (black dots) and by a brute force unbiased trajectory (triangles). The agreement is excellent. Also shown as circles are the steady state nonequilibrium probabilities π_α^A of the twisted dynamics. Note that by construction $\pi_{36}^A = 0$ (since $B_{36} = B$) and we did not plot this point.

are within statistical errors of the corresponding values obtained by the brute force simulation. Also shown in Fig. 5 are the probabilities π_α^A computed by twisting the dynamics. As expected, the closer to B , the smaller π_α^A is compared to π_α .

Acknowledgements. This work was motivated by a question from Benoit Roux. Partial support by NSF grants DMS02-09959, DMS02-39625 and DMS07-08140, and ONR grant N00014-04-1-0565 is also acknowledged.

* Electronic address: eve2@cims.nyu.edu

† Electronic address: mventuro@cims.nyu.edu

¹ A. Warmflash, P. Bhimalapuram, and A. R. Dinner, J. Chem. Phys. **127**, 154112 (2007).

² A. Dickson, A. Warmflash, and A. R. Dinner, J. Chem. Phys. **130**, 074104 (2009).

³ W. E and E. Vanden-Eijnden, J. Stat. Phys. **123**, 503 (2006).

⁴ E. Vanden-Eijnden, Transition path theory, in *Computer Simulations in Condensed Matter: From Materials to Chemical Biology - Vol. 1*, edited by M. Ferrario, G. Ciccotti, and K. Binder, pages 439–478, Berlin, 2006, Springer.

⁵ P. Metzner, C. Schütte, and E. Vanden-Eijnden, J. Chem. Phys. **125**, 084110 (2006).

⁶ E. Vanden-Eijnden and M. Venturoli, J. Chem. Phys. (2009), Accepted for publication.

⁷ A. K. Faradjian and R. Elber, J. Chem. Phys. **120**, 10880 (2004).

⁸ A. M. A. West, R. Elber, and D. Shalloway, J. Chem.

Phys. **126**, 145104 (2007).

⁹ R. Elber, Biophys. J. **92**, L85 (2007).

¹⁰ E. Vanden-Eijnden, M. Venturoli, G. Ciccotti, and R. Elber, J. Chem. Phys. **129**, 174102 (2008).

¹¹ D. Moroni, T. S. van Erp, and P. G. Bolhuis, Physica A **340**, 395 (2004).

¹² D. Moroni, P. G. Bolhuis, and T. S. van Erp, J. Chem. Phys. **120**, 4055 (2004).

¹³ T. S. van Erp and P. G. Bolhuis, J. Comput. Phys. **205**, 157 (2005).

¹⁴ R. J. Allen, D. Frenkel, and P. R. ten Wolde, J. Chem. Phys. **124**, 024102 (2006).

¹⁵ C. Valeriani, R. J. Allen, M. J. Morelli, D. Frenkel, and P. R. ten Wolde, J. Chem. Phys. **127**, 114109 (2007).

¹⁶ E. Vanden-Eijnden and M. Venturoli, J. Chem. Phys. (2009), Accepted for publication.

¹⁷ K. Mueller, Angew. Chem. **19**, 1 (1980).

¹⁸ E. Vanden-Eijnden and G. Ciccotti, Chem. Phys. Lett. **429**, 310 (2006).